Colloquia: SciNeGHE 2016

Modeling gravitational waves from compact-object binaries

A. Taracchini

Max Planck Institute for Gravitational Physics (Albert Einstein Institute)
Am Mühlenberg 1, Potsdam 14476, Germany

Summary. — The direct observation and characterization of gravitational waves from binary black-hole mergers by LIGO is a testament to the crucial role played by waveform modeling in these discoveries. I will review recent developments in the field, discussing both numerical and analytical approaches to the problem of black-hole binaries and their gravitational-wave emission.

1. – Binary black holes in general relativity

During its first observing run (O1), the Advanced Laser Interferometer Gravitational wave Observatory (LIGO) detected gravitational waves (GWs) emitted by the coalescence of two binary black holes (BBHs), GW150914 and GW151226 [1, 2]. A third candidate event, LVT151012, was also recorded [3], but with not high enough statistical significance to claim a detection. These discoveries opened the possibility of observing and probing the most extreme astrophysical objects in the Universe. These first detections and their detailed characterization represent the culmination of more than a decade of synergy between analytical relativity, numerical relativity (NR) and data analysis.

The problem of describing the GW signal generated by a pair of BHs that (quasi-circularly) orbit each other and eventually merge into a single BH is challenging because of the different dynamical regimes that this process spans. When the binary is wide —say, as compared to the BH horizons— the component objects move at orbital speeds (in the center-of-mass frame) that are small with respect to the speed of light. During this phase of the coalescence, the post-Newtonian (PN) (*i.e.*, slow-motion and weak-field) approximation to general relativity can be employed to model the orbital dynamics and the associated GW emission (see, *e.g.*, ref. [4] for an extensive review of the current status of PN theory applied to the two-body problem). As the BHs spiral in, plunge and eventually merge, their orbital motion becomes more relativistic and the GW energy flux is stronger. NR techniques are required to obtain highly-accurate waveforms during this stage of the process. State-of-the-art codes can now accurately evolve BBHs for several tens of orbits (~ 40–60) in large regions of the parameter space [5-11]: i) at large

mass ratios (~ 8), but for moderate BH (dimensionless) spin magnitudes (~ 0.6), and ii) at higher BH spin magnitudes, but for comparable masses (~ 1–3). Shorter simulations (~ 10) can also be produced for mass ratios ~ 20 and spin magnitudes ~ 0.8. The longest NR run to date covers 175 orbits of a nonspinning BBH with mass ratio 7 [12]. Finally, soon after the merger, a distorted remnant BH is born. This relaxes into a stationary Kerr spacetime by radiating GWs that are well described by BH perturbation theory, as well as by NR.

In spite of tremendous progress, a purely NR approach to simulating BBHs for any possible configuration down to the lower edge of the sensitive frequency band of current ground-based GW detectors is not feasible yet. This motivated the need to develop more sophisticated semi-analytical waveform models [13-17, 19, 20] that, while being cheap to compute for data analysis, are very good approximations to general relativity.

2. – Effective-one-body model

The effective-one-body (EOB) formalism [21] aims at combining all available results that describe the general-relativistic two-body problem — both analytical and numerical — into a unified description. In the case of a binary composed of BHs, let $m_{1,2}$ and $\boldsymbol{S}_{1,2}$ be the masses and spins of the two component objects as used in the PN description of the *real problem*. Let $q \equiv m_1/m_2 \geq 1$ be the mass ratio of the binary. The key ingredient of the EOB model is a resummation of the conservative PN dynamics of a generic BBH in terms of the conservative dynamics of a test particle with mass μ and spin $\boldsymbol{S}_*$ in a deformed Kerr metric with mass M and spin $\boldsymbol{S}_{\mathrm{Kerr}}$ (*effective problem*), the deformation parameter being μ/M. In analogy with the Newtonian treatment of a self-gravitating binary, here μ is the reduced mass of the BBH, while M is its total mass. As to the spins $\boldsymbol{S}_*$ and $\boldsymbol{S}_{\mathrm{Kerr}}$, these are given as functions of $m_{1,2}$, $\boldsymbol{S}_{1,2}$ and the dynamical variables [22, 23]. These relationships between mass and spin parameters of the real and effective problem are obtained imposing i) a precise energy mapping between the two systems, and ii) requiring that the Hamiltonian describing the effective problem reduces to that of the real problem in the slow-motion, weak-field limit. Concerning the dissipative sector, PN formulae for the inspiral GW modes are employed in a resummed form. The merger and ringdown signal is built independent of an orbital dynamics, namely by a superposition of quasinormal modes of the remnant BH or through fitting formulae. Strong-field information extracted from NR simulations can be incorporated into the model by calibrating adjustable parameters that enter the different ingredients of the model. The NR-informed versions of the EOB model go under the name of "EOBNR models".

3. – Recent results for spin-aligned BBHs

In ref. [20] we build an improved version of the spinning, nonprecessing EOBNR waveform model that was used for O1 [13, 14], and whose accuracy was recently found to degrade [24] in some regions of the BBH parameter space, notably large aligned spins and unequal masses, where the model was extrapolating away from the NR waveforms that were available at the time of its calibration. The improvements developed in this paper include: i) the addition of all 4PN terms to the EOB radial potential and of higher-order PN corrections to the polarization modes, ii) a recalibration of the EOBNR model to a large set of recently produced NR waveforms, which expand the domain of calibration towards larger mass ratios and aligned-spin components, and iii) a more robust
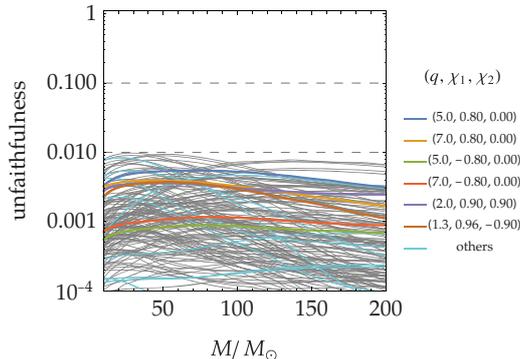
Fig. 1. – Unfaithfulness of the model of ref. [20] against the NR catalog used for its calibration + 16 additional validation runs for total masses $10\,M_\odot \leq M \leq 200\,M_\odot$, using the Advanced LIGO design zero-detuned high-power noise PSD and a low-frequency cutoff equal to the initial geometric frequency of each NR run.

description of the merger-ringdown signal. The updated model (SEOBNRv4) has been coded in the LIGO Algorithm Library, so that it can be employed during the second observing (O2) run of Advanced LIGO. One important figure of merit to determine the accuracy of a waveform model against a numerical-relativity simulation is the unfaithfulness, that is a frequency-domain overlap integral weighted by the noise power spectral density (PSD) of the detector of interest (in this case, zero-detuned high-power Advanced LIGO), with optimization only on phase and time of coalescence. Figure 1 shows that SEOBNRv4 has unfaithfulness below 1% against the whole NR catalog used for its calibration, with the addition of 16 validation runs. We compared the improved EOBNR model to spinning, nonprecessing waveform models that were used in the data analysis of the O1 run of Advanced LIGO, namely SEOBNRv2 [13] and IMRPhenomD [16]. IMRPhenomD is a frequency-domain waveform model that calibrates a phenomenological ansatz to NR waveforms hybridized with an uncalibrated version of the EOBNR model. We carried out faithfulness comparisons from 25 Hz with the O1 noise PSD. We found that SEOBNRv4 has faithfulness: i) as low as 43% against SEOBNRv2 in the region of large, positive aligned-spin components and spin-asymmetric BBHs, irrespective of the mass ratio, where new NR simulations became available for calibration; ii) as low as 35% against IMRPhenomD in the region of large, positive aligned-spin components and large mass ratios, where both models are extrapolating away from the respective calibration domain and the number of GW cycles in band is larger than in any other part of parameter space. The faithfulness results against IMRPhenomD waveforms at mass ratios > 4 and aligned-spin components > 0.8 strongly suggest the importance of producing new NR simulations in this region of the parameter space, so that discrepancies between different ways of extrapolating waveform models can be resolved. By contrast, the high effectualness between SEOBNRv4 and IMRPhenomD waveform models in almost all parameter space (both for O1 and design noise curves), suggests that for Advanced LIGO detection purposes the dominant-mode models do not need to be further improved.

4. – Recent results for spin-precessing BBHs

When the BH spins have generic orientations, both the orbital plane and the spins undergo precession about the total angular momentum of the binary. For the first time,

ref. [25] proposed a complete EOB model for spinning, precessing BBHs. The idea is to use a precessing frame that tracks the motion of the orbital plane [26]. In this frame, precession-induced amplitude and phase modulations in the waveforms are minimized, thus one employs a nonprecessing EOBNR model calibrated to NR to generate inspiral-plunge modes. The modes are then rotated to the inertial frame that is aligned with the spin of the remnant BH: in this frame, the merger-ringdown modes are generated and smoothly stitched to the rotated inspiral-plunge modes. Without recalibration of the underlying nonprecessing EOBNR model [27], the model was compared to two long, precessing NR simulations, finding very good agreement. Currently, the precessing EOBNR model is the only waveform model that includes all 15 parameters that characterize a BBH coalescence. In ref. [17], for the first time, we extensively tested the precessing EOBNR model against 70 NR simulations that span mass ratios from 1 to 5, dimensionless spin magnitudes up to 0.5, and generic spin orientations. While we did not recalibrate the inspiral-plunge signal of the underlying nonprecessing model, we improved the description of the merger-ringdown waveform. In particular, we included different QNMs according to the prograde/retrograde character of the plunge orbit and we prescribed the time of onset of the ringdown according to a robust algorithm that minimizes unwanted features in the amplitude of the waveforms around merger. We introduced a sky- and polarization-averaged unfaithfulness to meaningfully compare precessing waveforms. We devised a procedure to identify appropriate initial physical parameters for the model given a precessing NR simulation. We found that for Advanced LIGO the precessing EOBNR model has unfaithfulness within about 3% against the large majority of the 70 NR runs when the total mass of the binary varies between $10\,M_\odot$ and $200\,M_\odot$ and inclinations $\iota = 0, \pi/3, \pi/2$.

References [18, 15] proposed a precessing inspiral-merger-ringdown frequency-domain model based on the nonprecessing phenomenological model of ref. [16]. Similarly to what is done for the precessing EOBNR model, the inertial-frame waveforms are generated by rotating the nonprecessing modes according to the precessional motion of the orbital plane. The Euler angles parametrizing the rotation that connects the precessing frame to the observer's frame are derived from PN theory.

The precessing EOBNR model discussed in ref. [17] was one of the waveform models used in the parameter-estimation study of the first GW observation by LIGO, GW150914 [28]. Depending on the region of parameter space, the differences between the two precessing models may or may not be relevant. In particular, in the case of GW150914 —an almost equal-mass, face-off, non-extremal BBH — ref. [28] showed that both approximants give consistent estimations of the parameters of the source.

5. – Open problems

The nonprecessing (precessing) models discussed above only include the dominant (2,2) mode ($\ell = 2$ modes) in the GW polarizations $h_{+,\times}$. However, the inclusion of higher-order modes is likely to be important to increase our chance of detecting and correctly characterizing binary coalescences in some regions of the parameter space, notably large mass ratios [29-31]. Moreover, for spin-precessing binaries, some effects are still not accounted for by state-of-the-art models, namely mode asymmetry in the precessing frame [32-34] and the precession of the maximum-radiation direction during the ringdown [32]. Finally, no direct calibration of precessing waveform models to NR has ever been performed.

REFERENCES

[1] LIGO Scientific and Virgo Collaborations (Abbott B. P. *et al.*), *Phys. Rev. Lett.*, **116** (2016) 061102.

[2] LIGO Scientific and Virgo Collaborations (Abbott B. P. *et al.*), *Phys. Rev. Lett.*, **116** (2016) 241103.

[3] LIGO Scientific and Virgo Collaborations (Abbott B. P. *et al.*), *Phys. Rev. X*, **6** (2016) 041015.

[4] Blanchet L., *Living Rev. Rel.*, **17** (2014) 2.

[5] Mroue A. H. *et al.*, *Phys. Rev. Lett.*, **111** (2013) 241104.

[6] Chu T. *et al.*, *Class. Quantum Grav.*, **33** (2016) 165001.

[7] Lovelace G., Scheel M. A. and Szilagyi B., *Phys. Rev. D*, **83** (2011) 024010.

[8] Scheel M. A., Giesler M., Hemberger D. A., Lovelace G., Kuper K., Boyle M., Szilgyi B. and Kidder L. E., *Class. Quantum Grav.*, **32** (2015) 105009.

[9] Husa S., Khan S., Hannam M., Pürrer M., Ohme F., Jimnez Forteza X. and Boh A., *Phys. Rev. D*, **93** (2016) 044006.

[10] Jani K., Healy J., Clark J. A., London L., Laguna P. and Shoemaker D., *Class. Quantum Grav.*, **33** (2016) 204001.

[11] Healy J., Lousto C. O., Zlochower Y. and Campanelli M., arXiv:1703.03423 [gr-qc].

[12] Szilgyi B. *et al.*, *Phys. Rev. Lett.*, **115** (2015) 031102.

[13] Taracchini A. *et al.*, *Phys. Rev. D*, **89** (2014) 061502.

[14] Pürrer M., *Phys. Rev. D*, **93** (2016) 064041.

[15] Hannam M., Schmidt P., Boh A., Haegel L., Husa S., Ohme F., Pratten G. and Pürrer M., *Phys. Rev. Lett.*, **113** (2014) 151101.

[16] Khan S., Husa S., Hannam M., Ohme F., Pürrer M., Jimnez Forteza X. and Boh A., *Phys. Rev. D*, **93** (2016) 044007.

[17] Babak S., Taracchini A. and Buonanno A., *Phys. Rev. D*, **95** (2017) 024010.

[18] Schmidt P., Ohme F. and Hannam M., *Phys. Rev. D*, **91** (2015) 024043.

[19] Nagar A., Damour T., Reisswig C. and Pollney D., *Phys. Rev. D*, **93** (2016) 044046.

[20] Bohé A. *et al.*, *Phys. Rev. D*, **95** (2017) 044028.

[21] Buonanno A. and Damour T., *Phys. Rev. D*, **59** (1999) 084006.

[22] Barausse E. and Buonanno A., *Phys. Rev. D*, **81** (2010) 084024.

[23] Barausse E. and Buonanno A., *Phys. Rev. D*, **84** (2011) 104027.

[24] Kumar P. *et al.*, *Phys. Rev. D*, **93** (2016) 104050.

[25] Pan Y., Buonanno A., Taracchini A., Kidder L. E., Mrou A. H., Pfeiffer H. P., Scheel M. A. and Szilgyi B., *Phys. Rev. D*, **89** (2014) 084006.

[26] Buonanno A., Chen Y. b. and Vallisneri M., *Phys. Rev. D*, **67** (2003) 104025.

[27] Taracchini A. *et al.*, *Phys. Rev. D*, **86** (2012) 024011.

[28] LIGO Scientific and Virgo Collaborations (Abbott B. P. *et al.*), *Phys. Rev. X*, **6** (2016) 041014 doi:10.1103/PhysRevX.6.041014.

[29] Capano C., Pan Y. and Buonanno A., *Phys. Rev. D*, **89** (2014) 102003.

[30] Caldern Bustillo J., Laguna P. and Shoemaker D., arXiv:1612.02340 [gr-qc].

[31] Varma V. and Ajith P., arXiv:1612.05608 [gr-qc].

[32] O'Shaughnessy R., London L., Healy J. and Shoemaker D., *Phys. Rev. D*, **87** (2013) 044038.

[33] Pekowsky L., O'Shaughnessy R., Healy J. and Shoemaker D., *Phys. Rev. D*, **88** (2013) 024040.

[34] Boyle M., Kidder L. E., Ossokine S. and Pfeiffer H. P., arXiv:1409.4431 [gr-qc].